Synthesis and Characterization of Cu Doped ZnS Thin Films Deposited by Spin Coating

V.H. Choudapur[1,*], S.B. Kapatkar[1,†], A.B. Raju[2]

[1] *Department of Physics, B.V.B. College of Engineering and Technology , Hubballi, 580031, Karnataka, India*
[2] *Department of Electrical and Electronics Engineering, B.V.B. College of Engineering and Technology, Hubballi, 580031,Karnataka, India*

ZnS and copper doped zinc sulphide thin films are prepared through spin coating method. The nanoparticles are synthesized by hydrothermal method using low cost starting chemicals and demineralised water as solvent. The results of Cu doped zinc sulphide are compared with those of the undoped zinc sulphide. High band gap, uniform, and conducting thin films are obtained. The ultraviolet-visible absorption graphs were used to estimate the energy gap values. The XRD analysis verifies the successful addition of Cu atoms within the zinc sulphide lattice up to 6 % with no change in the host X-ray diffraction peak positions. However, the crystallinity is affected with Cu doping level in ZnS due to lattice strain. The XRD and EDS analysis of films confirm the purity of the samples. The films show high band gap, transparency, and electrical current in the range 10^{-4} to 10^{-11} mA. Adding Cu atoms to ZnS can tune the band gap and conducting properties. These are suitable for UV detectors and other optoelectronic applications.

Keywords: Spin coating, Hydrothermal method, Electrical resistivity, Cu doped ZnS thin films.

1. INTRODUCTION

Semiconductor nanomaterials are important materials as they find potential applications in most of the branches of science and technology. Semiconductor nanomaterials are unique due to their physical, chemical and optoelectronic properties, which depend on size of nanoparticles below a particular size which is the characteristic of that material. The semiconductor nanomaterials, particularly metal chalcogenides from the II-VI or III-VI and IV-VI groups, show quantum confinement effect. Zinc sulphide (ZnS) belonging to the II-VI groups is one of the widely known semiconductors discovered is considered as the developing and a potential material in various applications. It has a direct and wide band gap with two allotropic structures – one is cubic sphalerite structure having energy gap 3.72 eV and another is wurtzite hexagonal structure having energy gap 3.77 eV – and has large excitonic binding energy of 121 meV. Being more versatile, it exhibits effective transport properties, high charge carrier mobility and thermal stability etc. which result in rich ZnS nanostructures. These properties make ZnS to have a large number of applications, which include photodetectors, thermistors, gas sensors, a photo catalyst, field-emitters, antireflective coatings, alternative buffer layer for CZTS solar cells [1-3] etc. Zinc oxide is investigated in depth with widespread research developments than ZnS even though ZnS has a superior chemical and physical bulk property in comparison to ZnO [4]. Doping is a well-known method to tailor the energy band structures of a bulk semiconductor which in turn affects the material performance. It is understood from the current research work on semiconductor nanostructures that by introducing defects into the semiconductor lattices one can control the electrical resistivity and also influence the optical, structural,

luminescent, and other physical properties of the semiconductors. Amongst the II-VI semiconductor materials, the ZnS possesses chemical stability and technological importance as compared to other chalcogenides; as a result it can be a leading host material for doping. The transition metals such as Cu^{2+}, Mn^{2+}, Ag^{2+} , Eu^{2+}, Pb^{2+} etc. can be used to dope with ZnS to achieve interesting luminescence and tunability in the visible range of spectrum with good quantum yield [5]. Doped ZnS nanocrystals exhibit distinctive electronic and optical properties from that of bulk material. Many researchers have used transition metal ions Mn^{2+} and Cu^{2+} [6], rare earth elements, for example europium [7], and incorporated into ZnS nanostructures by either physical or chemical synthesis methods. The doped ZnS nanomaterials have a broad range of applications such as display systems, phosphors, electroluminescent devices, and optical sensors etc. The fabrication of nanomaterials is conducted by several methods like sol-gel processing [8], chemical spray coating [9], co-precipitation and chemical bath deposition [10] etc. Peng *et al.* studied Cu^{2+} doped nanoparticles by facile wet chemical method, exhibiting green emission which is basically related to the defect states by changing the Cu concentrations from 0-2 mol. %. Intrinsic ZnS nanoparticles show blue light emission due to the combined effect of emissions at 411 nm and 455 nm [11].

Corrado *et al.* carried out synthesis of Cu and Cl doped ZnS nanoparticles capped with mercaptopropionic acid (MPA) by aqueous route. These are well investigated by various techniques to reveal the effect of doping on optical and electronic properties [12]. The aqueous synthesis of the nanocrystals or quantum dots is ecofriendly, and synthesis under ambient conditions is more advantageous and green method as compared to organomettallic method [5]. Herein, we have synthesized Cu doped ZnS by green aqueous hydrothermal

* veena_choudapur@bvb.edu
† sbkapatkar@bvb.edu

method at different Cu concentrations and thin films through spin coating technique. The impact of Cu doping on ZnS structural and optoelectronic properties is investigated.

2. EXPERIMENTAL DETAILS

2.1 Chemicals Used

Zinc acetate, sodium sulphide and copper chloride of AR grade are obtained from Sd fine chemicals, India and are employed as received from industry.

2.2 Sample Preparation

ZnS nanocrystals are synthesized in a 100 ml capacity teflon coated cylindrical vessel placed in closed cylindrical chamber made of stainless steel. 30 ml of 0.7 M sodium sulphide and 30 ml of 0.3 M zinc acetate were dissolved in demineralized water and mixed under continuous magnetic stirring. Then, the reacted solution was quickly transferred to an autoclave. The autoclave is then placed in preheated 150 °C hot air oven precisely for 6 hours without disturbing. After 6 hours, oven was turned off and the autoclave was cooled naturally. The nanocrystals are washed a number of times with solvents through alternate ultrasonication and centrifugation till pH becomes neutral. ZnS nanocrystals are filtered and then dried at 70 °C in oven to get the powder form. This sample is named as 'A'. For Cu doping, $CuCl_2$ was added to the above precursor solution in the range 2 to 6 wt. % in comparison to zinc acetate. The doped samples are labeled as P, Q, and R with 2, 4, and 6 % of Cu doping in ZnS respectively. Firstly, the glass slides were cleaned by keeping in chromic acid. The glass slides are then boiled in soap solution and further cleaned using deionized water and acetone.

To prepare thin films, spin coating unit (Model spin NXG-p1, Apex India) was used with optimized spinning speed of 3000 rpm and 30 s. The intrinsic ZnS films and Cu:ZnS were deposited by spin coating. The spin coating is repeated eight to nine times for all the samples to get uniform, adherent, and compact films. The summery of samples and doping concentration values are listed in Table 1.

Table 1 – Summary of experimental conditions and results

Sample	Particle size from SEM, in nm	Crystallite size from XRD, in nm	Energy gap, in eV	Elecrical resistance, in ohms	Critical absorption, in nm
A	19.30	14.79	4.57	$1.1 \cdot 10^4$	271
P (2 % Cu)	42.53	42.40	4.20	$2.5 \cdot 10^9$	295
Q (4 % Cu)	74.21	61.1	3.95	$8.89 \cdot 10^9$	314
R (6 % Cu)	55.36	60	3.85	$2.29 \cdot 10^{10}$	323

2.3 Experimental Characterization

The XRD patterns of synthesized samples were obtained from STIC Cochin, India using X-Ray diffractometer (Bruker AXSD8Advance) operated at 1.5406 Å using CuKα radiation over a range of 20° to 90°. The SEM and EDS analysis were carried out by Centre for Nano Science and Engineering, IISc, Bangalore; UV-Visible absorption measurements were obtained in the

wavelength range 200-800 nm using UV-Visible-Near IR Spectrophotometer V-670 Jasco Int'l, Japan. *I-V* curves were obtained on films by homemade conductivity set up by two probe method with the use of Keithley-617 electrometers in room conditions.
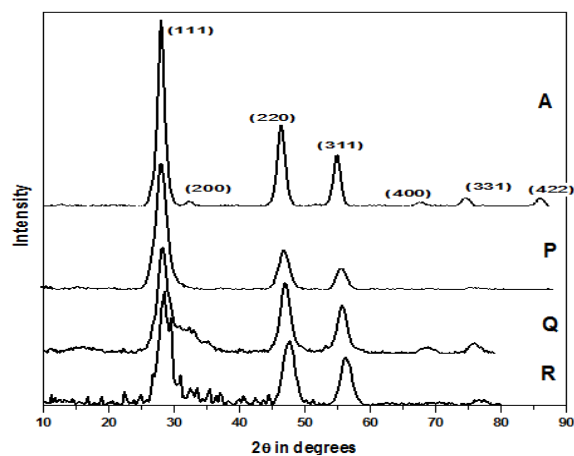

Fig. 1 – XRD patterns of Cu doped ZnS and undoped ZnS nanocrystallites

3. RESULTS AND DISCUSSION

3.1 X-Ray Diffraction Studies

The XRD spectra of intrinsic ZnS and Cu:ZnS nanoparticles are shown in Fig. 1. The undoped ZnS (sample A) spectra show high crystallinity and exhibit all the characteristic peaks (111), (200), (220), (311), (400), (331), and (422) of the cubic sphalerite phase of ZnS similar to standard database JCPDS No. 05-0566. Further, no additional peaks forming any secondary phases such as CuS, $Zn(OH)_2$ were observed signifying the pure form of ZnS phase. The Cu:ZnS spectra (samples P, Q and R) exhibit three characteristic peaks (111), (220), and (311) of polycrystalline nature with favored orientation along (111) direction. The undoped nanocrystals exhibit high crystallinity as compared to doped nanocrystals. With the increase in the Cu concentration from 2 to 6 % has influenced the crystallinity of intrinsic ZnS without any additional diffraction peaks of Cu impurities or CuS phase in doped P, Q, and R samples. This reveals that the copper ions are uniformly distributed into the ZnS lattice. P, Q, and R samples exhibit slight shifting of all peaks towards higher angles of diffraction as shown in Fig. 1, which is due to the lattice strain of dopants. These XRD results are consistent with the results presented by Mehrabian *et al.* [13]. The average crystallite size is calculated by using the Scherrer formula $D = 0.94\lambda / (\beta \cos\theta)$, where D is the average nanocrystallite size, $\lambda = 0.1506$ nm, θ is the angle of diffraction, and β is full width at half maximum of diffraction lines. The particle sizes of the samples are calculated and found to be in the range of 40 to 60 nm. The lattice parameter 'a' was calculated from equation, $a = d\sqrt{h^2 + k^2 + l^2}$, where '$d$' is the atomic spacing and h, k, and l are called Miller indices. The lattice constant is found to be 5.407 Å for the undoped ZnS as compared to the standard value 5.42 Å. For the doped samples, the lattice constant is 5.37 Å, comparatively lesser than the

standard value. The small change in the lattice constant is due to the substitution of copper ions onto zinc ion sites whose ionic radius (ionic radius of $Cu = 0.73$ Å) is greater than that of zinc ions (ionic radius of $Zn = 0.6$ Å) [14]. Srivastava *et al.* studied intrinsic ZnS and Cu:ZnS nanoparticles synthesized by simple co-precipitation method. XRD results show that ZnS nanoparticles are formed with sphalerite structure and at higher percentage of copper ions in ZnS, a secondary phase of copper sulphide (CuS) has been observed. The Cu:ZnS crystallites have size in the range of 2 to 4 nm [15].

a   b

c   d
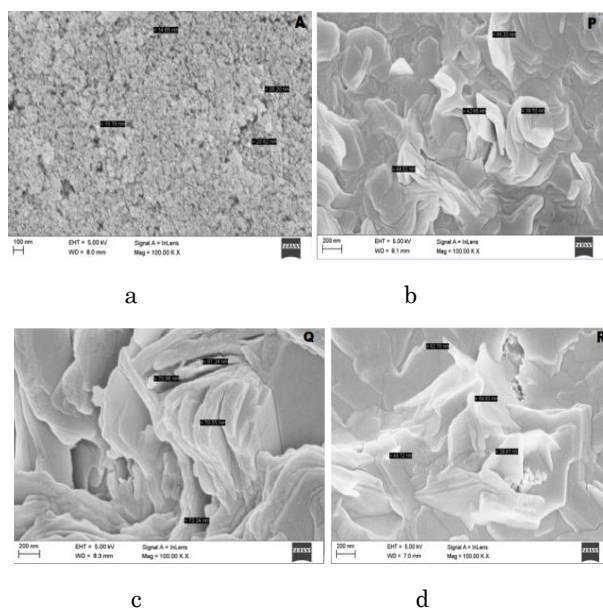
**Fig. 2** – Scanning electron micrographs of undoped ZnS (A) and Cu doped ZnS thin films (P, Q and R)

3.2 Scanning Electron Micrographs (SEM) and Chemical Analysis

Fig. 2 exhibits the surface morphology of the intrinsic ZnS and Cu doped ZnS films deposited at room temperature by spin coating method on glass substrate. It is observed that the doping concentration highly influences the surface morphology of the thin films. It is seen that the film 'A' contains continuous granules homogenously spread, compact, and adherent. The doped films exhibit clusters of nano-aggregate flakes formed by coalescence. With the increase in the copper percentage in ZnS, the small particulate structures changed to larger flakes. The nano-aggregates of large-size flakes distribution about 60 nm with average grain sizes are slightly greater than the estimated crystallite sizes as presented in Table 1. This is because of the fact that the grains are made up of crystallites. Similar grain distribution is observed by Muthukumaran *et al.* [14]. Chemical composition of the nanocrystals is investigated by EDS measurements. The results presented in Table 2 and shown in Fig. 2 indicate that all the films no longer contain impurity atoms. The chemical composition of undoped ZnS shows that the Zn atomic percentage is 78.63 and that of S is 21.37 and Zn/S atomic ratio is 3.67. This reveals that the Zn atoms are in excess and occupy either the interstitial sites or at their regular sites by creating equivalent number of

sulphur vacancies. In both cases the conductivity in intrinsic ZnS semiconductor changes. When the intrinsic ZnS is doped with Cu ions, these copper ions successfully occupy the Zn^{2+} sites reducing the Zn/S ratio close to 1 as summarized in the Table 2 that is even after doping, the Zn/S atomic ratio is maintained nearly equal to 1. This means that up to 6 % of Cu atoms can be easily substituted into the ZnS lattice by substitutional diffusion without altering the host crystal structure. The results discussed are consistent with S. Muthukumaran *et al.* [14].

Table 2 – Compositional analysis of different ZnS films by energy dispersive X-ray analysis

Thin film	Element	Atomic wt. %	Atomic ratio (Zn/S)
A	Zn/S	78.63/21.37	3.67
P	Zn/S Cu	58.02/41.98 2.00	1.38
Q	Zn/S Cu	51.98/48.02 2.14	1.082
R	Zn/S Cu	51.22/45.37 3.42	1.13

a   b

c   d
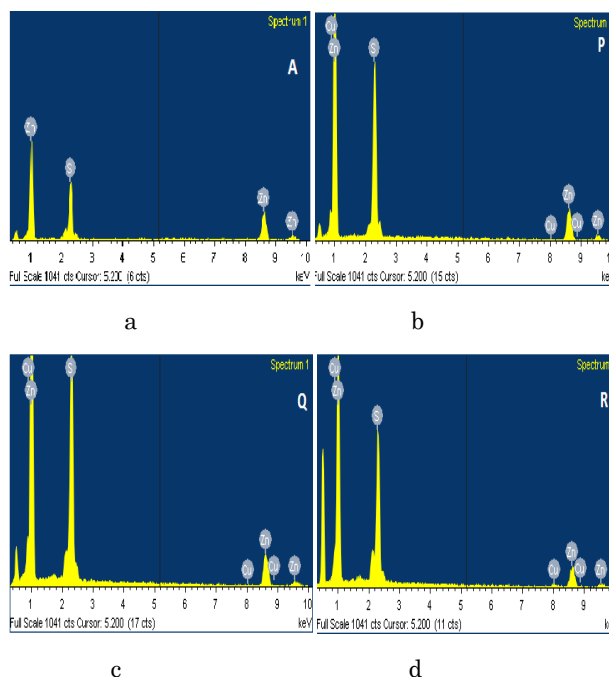
Fig. 3 – Energy dispersive spectroscopy spectra of intrinsic ZnS (sample A) and Cu doped ZnS (P, Q and R)

3.3 UV-Visible Absorption Analysis

Fig. 4a shows the UV-visible absorption spectra of intrinsic ZnS and 2, 4, and 6 % copper doped ZnS nanomaterial dispersed in solvent respectively in the wavelength range of 200 and 800 nm. Intrinsic film is highly transparent (Fig. 4) and the doped films are light green color, their transparency decreases as Cu concentration increases. For all the samples, the maximum absorption is seen in the ultraviolet region due to the quantum size effect. Absorption curve of undoped ZnS shows its energy gap transition close to 270 nm in accord with the optical gap (E_g) of 4.57 eV. The doped ZnS films formed at dif-

ferent concentrations of copper show the characteristic optical energy gap transition between 271 to 322 nm corresponding to energy gap between 3.85 to 4.57eV. Doped films exhibit an uneven red shift in the absorption peak which is very sharp for 4 and 6 % doped films. All these absorption peaks lie in UV region of 200 to 300 nm range. The optical absorption coefficient a can be obtained from an optical density A by using the formula $a = 2.303 \cdot (A/t)$, where t is the width of sample under illumination, A is the absorbance or optical density which is given by the equation $A = \log(I_0/I)$, where I and I_0 are the transmitted and incident intensities of the light, respectively. The transmitted intensity can be written as $I = I_0 \exp(-\alpha)$. The absorption coefficient α is related to incident photon energy $(h\nu)$ by $(\alpha h\nu)^n = B(h\nu - E_g)$,where 'B' is constant, E_g is energy gap, and $n = 2$ for direct band gap semiconductors. The direct energy gap E_g for the intrinsic ZnS and Cu:ZnS are obtained by extending linear portion of the $(\alpha h\nu)^2$ vs $h\nu$ graph up to the x-axis as shown in Fig. 5. The intersection value at x-axis gives energy gap of the samples. These energy gap values are tabulated in Table 1. It is noticed that the undoped ZnS band gap energy is more than that of Cu:ZnS material and as Cu concentration increases, the E_g value decreases. Similar changes in band gap are reported by researchers of [11]. According to some authors, for Cu doped ZnS, an absorption shoulder is formed at 319 nm for intrinsic ZnS nanoparticles and for bulk zinc sulphide it is reported to be formed at 336 nm in contrast to the 4 % Cu doped sample, which shows 309 nm absorption edge. The blue shift of absorption shoulder is due to the quantum size effect [15]. Gang-Juan Lee *et al*. synthesized Cu:ZnS by sonochemical method, reported that the absorption edge is red shifted for the hollow Cu:ZnS nanostructures and justified the results due to Cu ions substituted by Zn ions [16]. Highly transparent, *p*-type conductive Cu:ZnS films by chemical bath deposition and the absorption spectra of Cu:ZnS with increase in Cu content in ZnS, demonstrate continuous red shift in the absorption edge [17].

3.4 Photoluminescence (PL) Studies

Fig. 6 shows the PL spectra of ZnS and Cu:ZnS nanoparticles which are performed at room temperature. The PL spectra of intrinsic ZnS and Cu:ZnS are broad and asymmetric. At an excitation wavelength of 373 nm, the PL spectra (Fig. 6a) of pure ZnS show two peaks: first peak at 408 nm associated with UV light emission and second peak at 431 nm associated with the blue emission. The peaks at 408 nm and 431 nm correspond to violet blue range due to deexcitation of photoexcited electrons onto zinc interstitial sites and sulphur vacancy sites. PL Spectra peak of Cu:ZnS appears at the 465 nm when performed at excitation wavelengths of 215 nm, 268 nm and 262 nm for P, Q and R. So there is a red shift in PL peak occurrence from 408 nm wavelength range of intrinsic ZnS peaks showing large difference of peak intensities. The luminescence intensity is diminished as Cu concentration in ZnS increases. More number of defect states will be created when copper ions are introduced into ZnS lattice, and these defect states will result into poor peak intensities. These low peak intensities are defect related recombination between the sul-
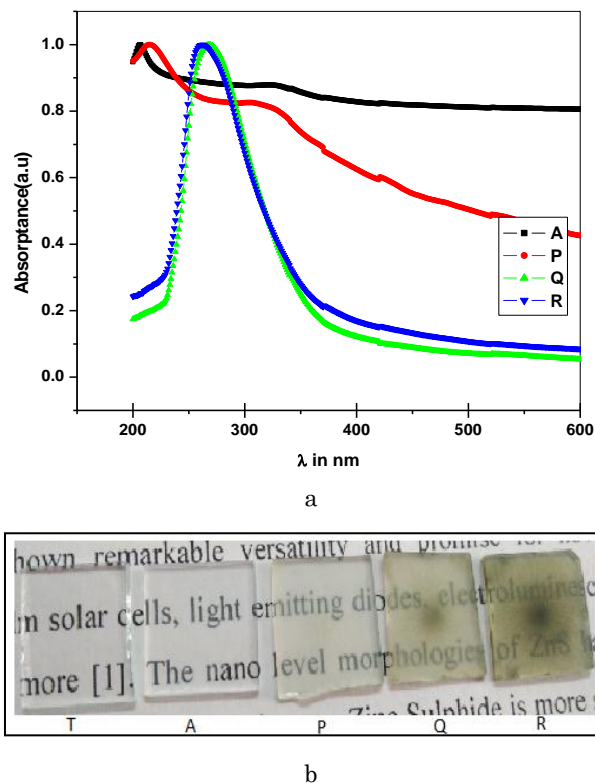

Fig. 4 – UV-Vis absorption spectra of Cu doped ZnS and undoped ZnS (a) and photos of thin films coated on glass slide by spin coating: T – uncoated transparent glass; A – Intrinsic ZnS; P, Q, and R – Cu doped ZnS films (2, 4 and 6%) (b)
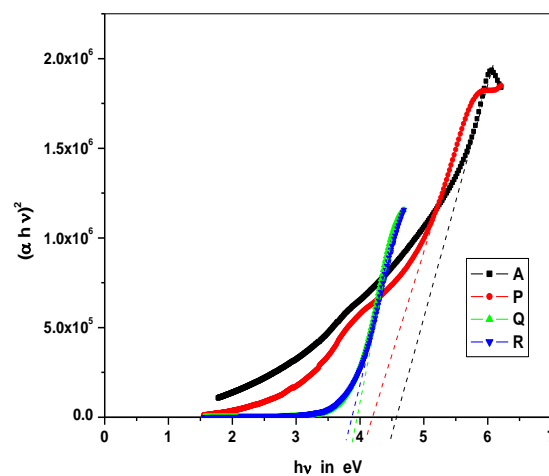

Fig. 5 – The graph of $(\alpha h\nu)^2$ against photon energy $h\nu$
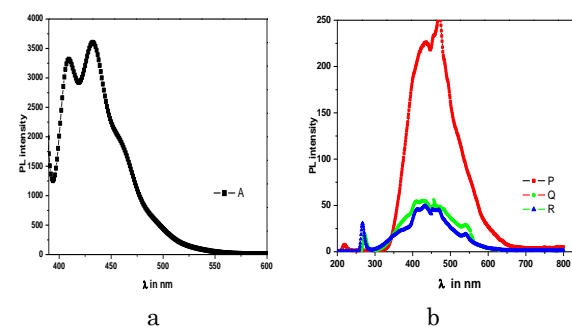

Fig. 6 – Fluorescence spectra of intrinsic ZnS (a) and Cu doped ZnS (b)

phur vacancy donor and valence band. Similar observations are reported by S. Sambasivam *et al.* [18].

3.5 Electrical Properties

Current-voltage characteristics of ZnS and Cu:ZnS were measured for the films deposited on indium tin oxide (ITO) coated glass slides using the home made special set up to measure electrical conductivity by two probe technique with soft electrical contacts. Fig. 7 shows semi-logarithmic current-voltage curves for Cu doped and undoped ZnS films. The curves of all four thin films reveal a linear relationship, and therefore all films are Ohmic in nature for the entire measurement range. It is observed from these plots that for voltage of 1 V, the current in intrinsic film is of the order of 10^{-4} A and that in doped films is of the order of 10^{-10} A. Almost five orders of difference have been observed for intrinsic and doped films for the same voltage. From these data, electrical resistances were estimated for all films and the data is summarized in Table 1. The drastic variation in the resistance may be understood in two ways. One main reason is the difference in E_g value of the doped and undoped films and another thing is charge transport mechanism and free carrier absorption with respect to the dopants, which create the additional electronic states in their band gap. The resistivity of doped films is high. In this case, it has been observed that lower energy band gap, poor crystallinity and free carrier absorption in doped films result in high electrical resistance. The poor crystallinity and its polycrystalline nature lead to the formation of grain boundaries and hence reducing the mobility of electrons. These reports are in accord with other results [13]. Oztas *et al.* [19] conducted the IV characteristics of ZnS thin films using a Van der Pauw four-probe method. The Cu doped ZnS has high resistance (10^5 to 10^7 $\Omega \cdot$cm) compared to intrinsic ZnS films which have resistance in the range of $1.5 \cdot 10^4$-$1.7 \cdot 10^6$ Ωcm when the temperature of substrate varied from 400 °C to 500 °C. These resistance values are in good agreement with our results. However, the obtained results are inconsistent with Goktas *et al.* [20] reported that the resistivity for Cu:ZnS films prepared by wet chemical dip coating route at room temperature, decreased from $5.61 \cdot 10^5$ to $4.72 \cdot 10^3$ $\Omega \cdot$cm by increasing Cu doping concentration from 10 to 20 %. In this case, the crystallinity improved with Cu doping in ZnS is reported, hence the resistivity of 10 to 20 % Cu doped ZnS films decreases.

Fig. 7 – Semi-logarithmic IV curves of Cu doped ZnS and intrinsic ZnS thin films

4. CONCLUSIONS

The ZnS and Cu doped ZnS nanoparticles are synthesized by green hydrothermal method. Uniform, adherent and conducting thin films are obtained by simple spin coating. The X-ray diffraction studies show that the Cu ions are well dispersed into the ZnS lattice without changing the host crystal structure. The optical band gap decreased after doping Cu into ZnS from 4.57 to 3.85 eV. It is observed that the transparency and conductivity change significantly with the Cu concentration in ZnS due to free carrier absorption and diffused crystallinity. The EDS analysis confirms that nanocrystals are free from impurities, and doped materials contain copper atoms 2, 2.14 and 3.42 % by weight in ZnS. The intrinsic ZnS thin film is found to be more transparent and conducting of the order of 10^{-4} mA and Cu doped ZnS films have lower band gap and conducting of the order of 10^{-11} mA. These have applications in high frequency UV light detectors, electroluminescent and optoelectronic devices.

REFERENCES

1. Xiaosheng Fang, Tianyou Zhai, U.K.Gautam, Liang Li, Limin Wu, Yoshio Bando, Dmitri Golberg, *Prog. Mater. Sci.* **56**, 175 (2011).
2. Xiaosheng Fang, Limin Wu, Linfeng Hu, *Adv. Mater.* **23**, 585 (2011).
3. Xiaosheng Fang, Yoshio Bando, Ujjal K. Gautam, Changhui Ye, Dmitri Golberg, *J. Mater. Chem.* **18**, 509 (2008).
4. He Hu, Weihua Zhang., *Opt. Mater.* **28**, 536 (2005).
5. Mohammad Hussain K. Rabinal, Raghu M. Gunnagol, Rajashree M. Hodlur, *Curr. Nanomater.* **1**, 12 (2016).
6. Niladri S. Karan, D.D. Sarma, R.M. Kadam, Narayan Pradhan, *J. Phys. Chem. Lett.* **1**, 2863 (2010).
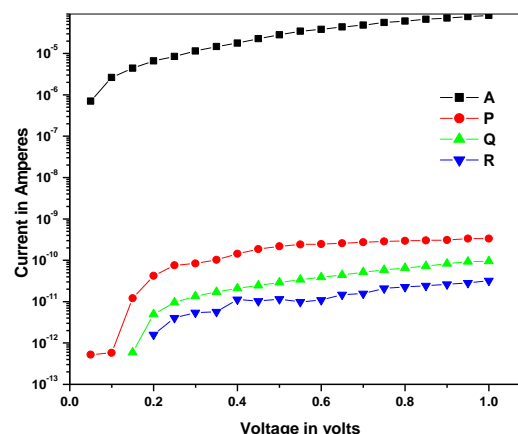7. M.J. Rivera-Medina, J. Hernandez-Torres, J.L. Boldu-Olaizola,

J. Barreto-Renteria, J. M.Hernandez-Alcantara, V. Jancik, J.C. Alonso-Huitron, *RSC Adv.* **6**, 107613 (2013).
8. H.K. Sadekar, N.G. Deshpande, Y.G. Gudage, A. Ghosh, S.D. Chavhan, S.R. Gosavi, Ramphal Sharma, *J. Alloys Compd.* **453**, 519 (2008).
9. P.O. Offor, B.A. Okorie, F.I. Ezema, V.S. Aigbodion, C.C. Daniel-mkpume, A.D. Omah, *J. Alloys Compd.* **650**, 381 (2015).
10. Seung Wook Shin, G.L. Agawane, Myeng Gil Gang, A.V. Moholkar, Jong-Ha Moon, Jin Hyeok Kim, Jeong, Yong Lee, *J. Alloys Compd.* **526**, 25 (2012).
11. W.Q. Peng, G.W. Cong, S.C. Qu, Z.G.Wang, *Opt. Mater.* **29**, 313 (2005).

12. Carley Corrado, Yu Jiang, Fadekemi Oba, Mike Kozina, Frank Bridges, Jin Z. Zhang, *J. Phys. Chem. A* **113**, 3830 (2009).
13. M. Mehrabian, Z. Esteki, H. Shokrvash, G. Kavei, *J. Semicond.* **37**, 10 (2016).
14. S.Muthukumaran, M.Ashokkumar, *Mater. Lett.* **93**, 223 (2013).
15. Rajneesh K. Srivastava, Nitin Pandey, Sheo K. Mishra, *Mater. Sci. Semicond. Process.* **16**, 1659 (2013).
16. Gang-Juan Lee, Sambandam Anandan, Susan J. Masten, Jerry J. Wu, *Ind. Eng. Chem. Res.* **53**, 8766 (2014).
17. Xiaojie Xu, James Bullock, Laura T. Schelhas, Elias Z. Stutz, Jose J. Fonseca, Mark Hettick, Vanessa L. Pool, Kong Fai Tai, Michael F. Toney, Xiaosheng Fang, Ali Javey, Lydia Helena Wong, Joel W. Ager, *Nano Lett.* **16**, 1925 (2016).
18. S. Sambasivam, B. Sathyaseelan, D. Raja Reddy, B.K. Reddy, C.K. Jayasankar, *Spectrochim. Acta A* **71**, 1503 (2008).
19. Mustafa Oztas, Metin Bedir, A. Necmeddin Yazici, E. Vural Kafadar, Hu seyin Toktamıs, *J. Phys B.* **12**, 248 (2006).
20. A.Goktas, F.Aslan, A.Tumbul, *J. Sol-Gel Sci. Technol.* **75**, 45 (2015).

Синтез та характеристики тонких плівок ZnS, легованих Cu, осаджених методом центрифугування

V.H. Choudapur[1], S.B. Kapatkar[1], A.B. Raju[2]

[1] *Department of Physics, B.V.B. College of Engineering and Technology , Hubballi, 580031, Karnataka, India*
[2] *Department of Electrical and Electronics Engineering, B.V.B. College of Engineering and Technology, Hubballi, 580031, Karnataka, India*

Тонкі плівки чистого ZnS та ZnS, легованого міддю, виготовлені методом центрифугування. Наночастинки синтезуються гідротермальним методом, використовуючи недорогі вихідні хімікати та демінералізовану воду як розчинник. Результати для сульфіду цинку, легованого Cu, порівнюються з результатами нелегованого сульфіду цинку. Отримані однорідні та провідні тонкі плівки з великим значенням ширини забороненої зони. Графіки поглинання в ультрафіолетовому та видимому діапазонах використовувались для оцінки значень ширини забороненої зони. Аналіз рентгенівських досліджень підтверджує успішне додавання атомів Cu в решітку сульфіду цинку до 6 % без зміни позицій піків рентгенівської дифракції матриці. Однак на кристалічність впливає рівень легування Cu в ZnS через деформації решітки. XRD та EDS аналіз плівок підтверджує чистоту зразків. Зразки демонструють великі значення ширини забороненої зони, прозорість та електричний струм у діапазоні від 10^{-4} до 10^{-11} мА. Додавання атомів Cu до ZnS може змінювати ширину забороненої зони та провідні властивості. Такі плівки підходять для УФ-детекторів та інших оптоелектронних застосувань.

Ключові слова: Метод центрифугування, Гідротермальний метод, Електричний опір, Тонкі плівки ZnS леговані Cu.